BACKWARD-FACING STEP FLOW BETWEEN STEP-SIDE STATIONARY AND MOVING WALLS

Youhei Morinishi
Department of Mechanical Engineering,
Nagoya Institute of Technology
Gokiso-cho, Showa-ku, Nagoya, 466-8555, Japan
youhei.morinishi@nitech.ac.jp

ABSTRACT

Turbulent flows over a backward-facing step in a channel between the step-side stationary and the moving walls have been studied experimentally. Three non-dimensional parameters that specify the flow condition are the channel expansion ratio (ER), the Reynolds number ($Re_{\tau 0}$), and the flow type parameter (β_0, non-dimensionalized pressure gradient). In this study, the channel expansion ratio and the Reynolds number are fixed at $ER=1.5$ and at $Re_{\tau 0}=300$, respectively, in order to explore the effect of the pressure gradient on the velocity profile. With the hot-wire measurement, the profiles of mean velocity and fluctuation intensity have been analyzed. The logarithmic and the half-power laws for the mean velocity have been detected in the redevelopment region.

INTRODUCTION

The backward-facing step flow is one of the most fundamental flows with separation and reattachment, and a lot of researches have been conducted (Eaton and Jhonston, 1981) for engineering interest. The flow between the parallel walls with fully developed upstream, in particular, is characterized by the channel expansion ratio, the upstream Reynolds number, and the upstream non-dimensional pressure gradient. However, the effect of the upstream non-dimensional pressure gradient has hardly been investigated. It is known that the Reynolds number and the non-dimensional pressure gradient can be set independently in the flow between the stationary and the moving parallel walls (El Telbany and Reynolds, 1980, Nakabayashi et al., 2004). In this study, the turbulent flows over a backward-facing step in the channel between the step-side stationary and the moving walls (Fig.1) have been studied experimentally, in order to set the non-dimensional pressure gradient arbitrarily. The velocity profiles have been measured with the hot-wire velocimetry, and the laws for the mean velocity in the redevelopment region have been considered.

OUTLINE OF THE FLOW AND EXPERIMENTAL APPARATUS

Figure 1 shows the outline of the backward-facing step flow and experimental conditions. Upstream channel flows are Couette-Poiseuille type turbulent flows fully developed with different streamwise pressure gradients. Three non-dimensional parameters that specify the flow condition are the channel expansion ratio, the friction Reynolds number

Table 1: Flow conditions, reattachment ant secondary separation points

Case	β_0	Re_{τ_0}	ER	x_R/H	x_{SS}/H
P300	-1.0	300	1.5	6.50 ± 1.75	2.00 ± 0.50
CP300	-0.5	300	1.5	6.50 ± 1.50	2.00 ± 0.50
C300	0.0	300	1.5	6.63 ± 1.38	1.88 ± 0.38

defined by $Re_{\tau 0} = u_{\tau 0} H/\nu$, and the flow type parameter defined by $\beta_0 = H(dp/dx)_0/(\rho u_{\tau 0}^2)$. Here H is the channel half width, $u_{\tau 0}$ is the friction velocity on the stationary wall, and $(dp/dx)_0$ is the streamwise pressure gradient, where the values with subscript 0 are at at the upstream channel. ρ and ν are density and kinematic viscosity of fluid, respectively. The remarkable merits of the present flow are that the combination of the Reynolds number and the flow type parameter can be set arbitrarily in the fully developed upstream channel flow while the flow type parameter is fixed at -1 for the flow between the stationary walls.

Table 1 shows the flow conditions for three cases that appear in this study. Upstream flows for Cases P300, CP300, and C300 are the fully developed pure Poiseuille flow ($\beta_0=-1$), the Couette-Poiseuille flow at $\beta_0 = -0.5$, and the pure Couette flow ($\beta_0=0$), respectively. The friction Reynolds number, $Re_{\tau 0}$, is 300. The channel expansion ratio, ER, is 1.5, which indicates that the step height is equal to the upstream channel half width, H.

Figure 2 shows the schematic of experimental apparatus, which is composed of the step-side stationary wall with a step height of 15.05mm, the moving belt, and the side walls. The inlet of the channel is connected with an air blower through a diffuser and a two-dimensional nozzle. The lengths of upstream and downstream channels, L_1 and L_2, are 2500 and 2300mm, respectively, and the spanwise channel width, W, is 865mm. The values of $Re_{\tau 0}$ and β_0 are set by adjusting the flow rate of the blower, Q, and the belt speed, U_b.

RESULTS AND DISCUSSIONS

Figures 3 and 4 show the pressure coefficient, $C_{p\tau} = 2(p - p_{ref})/(\rho u_{\tau 0}^2)$, on the stationary wall, where p_{ref} is the static pressure at $x = -0$. The streamwise gradients of $C_{p\tau}$ upstream of the step agree with the given $2\beta_0$ values, that is, $dC_{p\tau}/d(x/H)=2\beta_0 = -2, -1$, and 0 for Cases P300, CP300, and C300, respectively. The linear distributions of $C_{p\tau}$ indicate that the upstream flows are fully developed. The development of the upstream flows is also verified by the
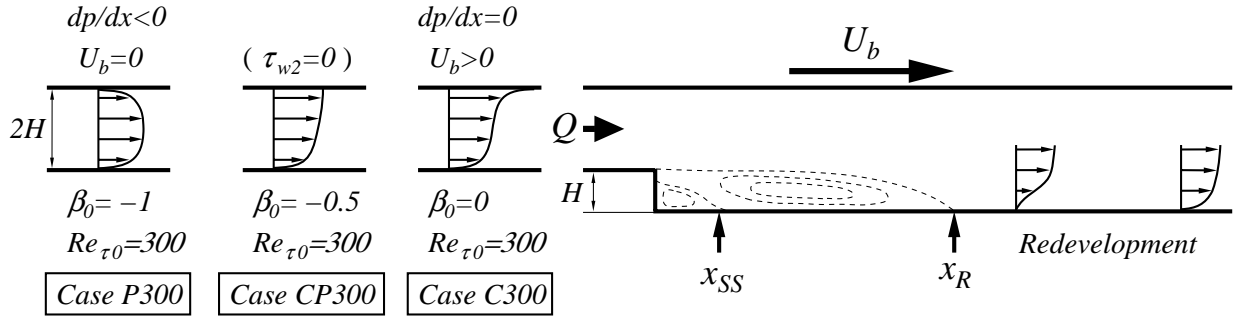
Figure 1: Backward-facing step flow between step-side stationary and moving walls

Table 2: Upstream and local non-dimensional parameters

Case	x/H	$Re_{\tau 0}$	β_0	Re_τ	β
P300	5	292.0	-1.000	—	—
	10	293.2	-1.000	306.8	4.533
	12	293.0	-1.000	281.8	2.581
	15	293.5	-1.000	305.5	0.930
	17	295.1	-1.000	279.0	0.272
	20	290.7	-1.000	279.9	-0.245
	30	293.0	-1.000	275.2	-0.902
	50	294.1	-1.000	301.6	-0.926
CP300	5	300.5	-0.434	—	—
	10	300.8	-0.430	256.6	9.725
	12	299.9	-0.445	258.1	6.633
	15	300.1	-0.444	278.6	3.213
	17	300.2	-0.477	306.4	2.359
	20	299.8	-0.444	253.1	2.438
	30	299.5	-0.445	252.3	1.063
	50	300.2	-0.457	287.2	0.258
C300	5	300.0	0.020	—	—
	10	300.1	0.060	257.0	11.408
	12	300.0	0.046	284.4	7.187
	15	300.2	0.056	267.2	5.516
	17	299.8	-0.003	290.6	3.690
	20	300.0	0.006	266.1	4.184
	30	300.4	0.018	289.2	2.574
	50	300.1	0.029	285.8	1.985

velocity measurement. The pressure gradient in the downstream region far from the reattachment point is adverse for Case C300, while it is favorable for Cases P300 and CP300. The reattachment and secondary separation points, x_R and x_{SS}, were specified by the tuft visualization method. The central point of the reattachment region is hardly dependent on β_0 as shown in Table 1. As β_0 increases, the fluctuation amplitude of the reattachment point slightly decreases.

The velocity was measured by I-type hot-wire velocimetry on the sections at $x/H = -20, 5, 10, 12, 15, 17, 20, 30, 50$. The measurements resolve the viscous sub-layer for specifying the local friction velocity, u_τ, except for the section with separation ($x/H = 5$). The effect of radiation from the wall is compensated for by the method of Bhatia et al. (1982). Figure 5 shows the mean streamwise velocity (U) profiles normalized by the bulk velocity (U_{m0}) at the upstream section ($x/H = -20$). From the velocity profiles close to the step-side wall, the values of the local friction velocity (u_τ) are determined at each section. Table 2 shows the upstream and local non-dimensional parameters, where $Re_\tau = u_\tau H/\nu$ and $\beta = H(dp/dx)/(\rho u_\tau^2)$ are the local friction Reynolds number and the local flow type parameter, respectively.

The mean velocity profiles are scaled in the local wall coordinates as $U^+ = U/u_\tau$ and $y^+ = y/\delta_v$ and they are shown in Fig. 6, where $\delta_v = \nu/u_\tau$ is the local viscous length scale. The region for the logarithmic velocity law,

$$U^+ = \frac{1}{k} \log y^+ + C \tag{1}$$

is marked as rectangular symbols in the figure. The formation of the logarithmic law is detected in the region where the value of $y^+ dU^+/dy^+$ is constant. The logarithmic law of velocity is observed even on sections just after the reattachment region. The additive constant (C) that appears in the logarithmic law decreases as β_0 increases in the redevelopment region.

The half power law,

$$U^+ = K_1 \left(\frac{y}{\delta_p} \right)^{1/2} + K_2 \tag{2}$$

is known as the mean velocity law for flows subject to the adverse pressure gradient, where $U^+ = U/u_\tau$ and $\delta_p = \rho u_\tau^2/|dp/dx|$. K_1 and K_2 are constants. The formation of the half-power law is detected in the region where the value of $(y/\delta_p)^{1/2}(dU^+/d(y/\delta_p))$ is constant. Figure 7 shows the mean velocity profiles on sections with the adverse pressure gradient. The region for the half-power law is marked as rectangular symbols in the figure. The half-power law is formed in the fore part of the redevelopment region for the flows with $\beta_0 = -0.5$ and 0, while it is not observed for the flow with $\beta_0 = -1$.

The streamwise turbulent intensity profiles in the redevelopment region are plotted in the wall coordinates in Fig.8. The DNS data of the plane turbulent channel flow (Morinishi et al., 2002) with $Re_\tau = 300$ and $\beta = -1$ are also plotted for reference. In the region very close to the wall ($y^+ < 10$), u'^+ is proportional to y^+ and slightly increases as β_0 increases.

REFERENCES

Bhatia, J. C., Durst, F. and Jovanovic, J., 1982, "Correction of hot-wire anemometer measurements near wall", *J. Fluid Mech.*, Vol. 122, (1982), pp.411-431.

Eaton, J. K. and Johnston, J. P., 1981, "A review of research on subsonic turbulent flow reattachment", *AIAA J.*, Vol. 19, pp.1093-1100.

El Telbany, M. M. M. and Reynolds, A. J. J., 1980, "Velocity distribution in plane turbulent channel flows", *J. Fluid Mech.*, Vol. 100, pp. 1-29.

Morinishi, Y., Nakabayashi, K., Okumura, T., 2002, "Turbulence statistics near the wall with almost zero shear stress", *Trans. JSME, Series B*, Vol. 68, pp. 2261-2268.

Nakabayashi, K., Kitoh, O. and Kato, Y., 2004, "Similarity laws of velocity profiles and turbulence charasteristics of Couette-Poiseuille turbulent flows", *J. Fluid Mech.*, Vol. 507, pp. 43-69.
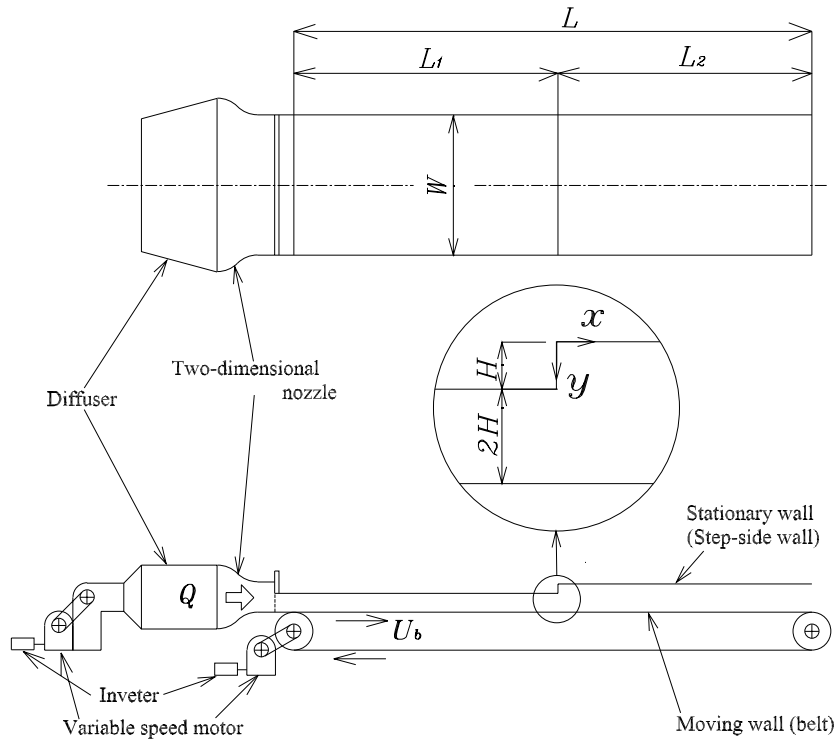
Figure 2: Experimental apparatus
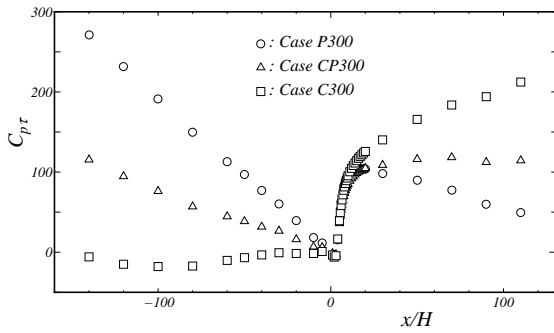
Figure 3: Distribution of $C_{p\tau}$
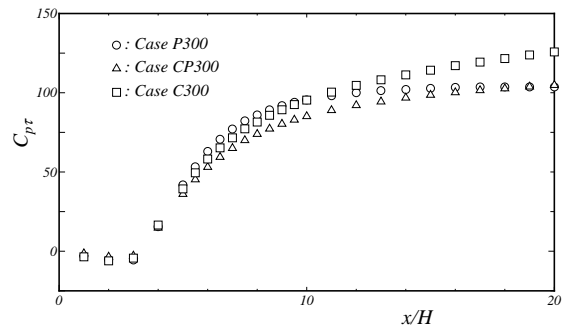
Figure 4: Distribution of $C_{p\tau}$ close to the step
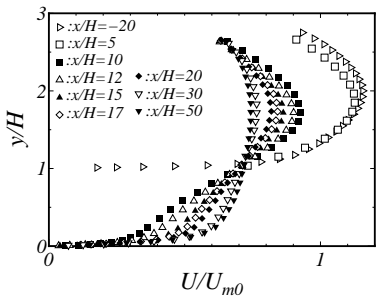
(a) Case P300
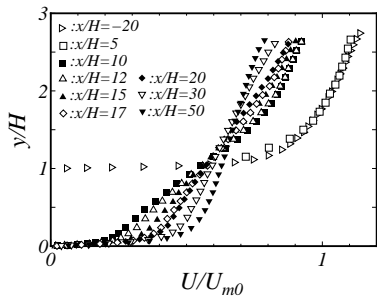
(b) Case CP300
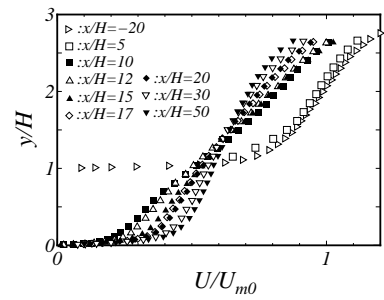
(c) Case C300

Figure 5: Mean velocity profiles
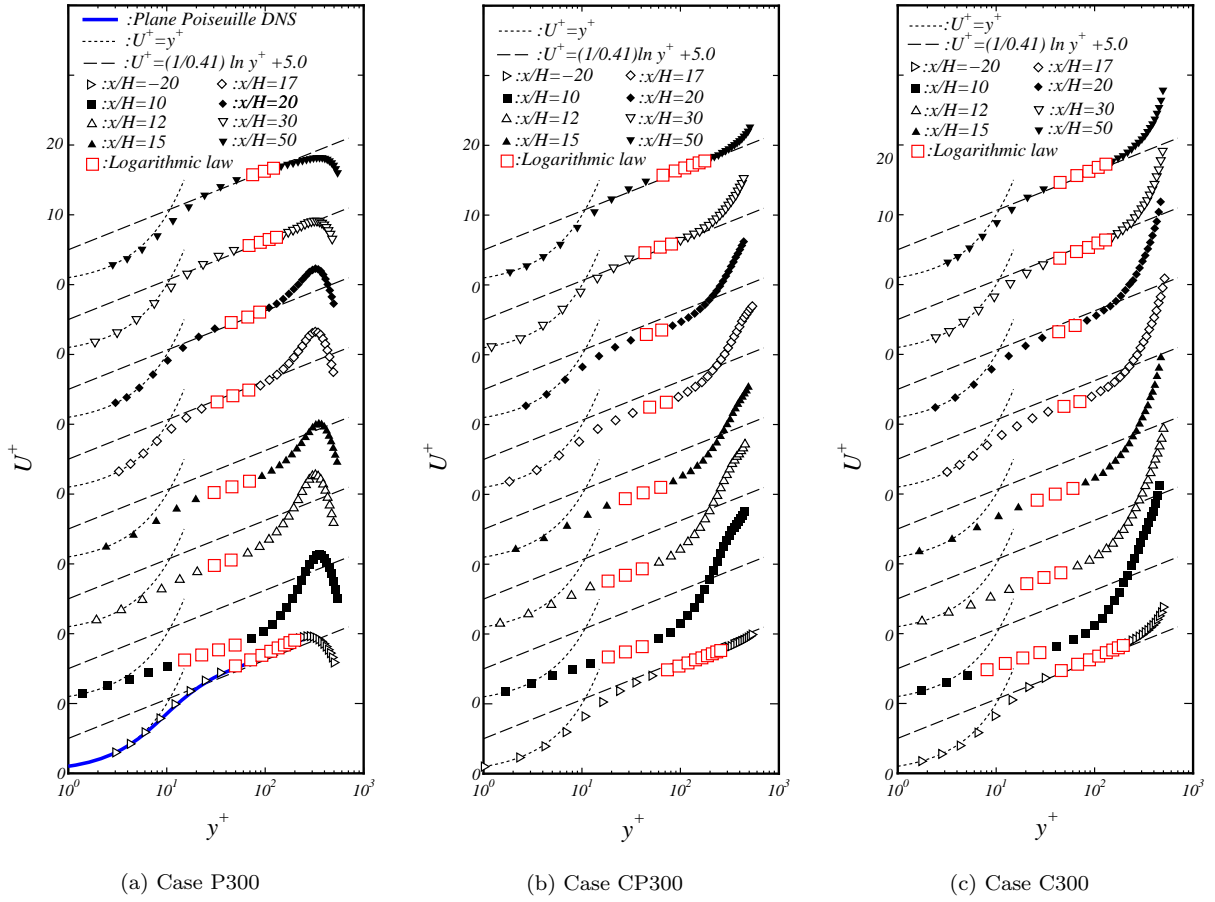
Figure 6: Mean velocity profiles in wall coordinates

(a) Case P300

(b) Case CP300

(c) Case C300
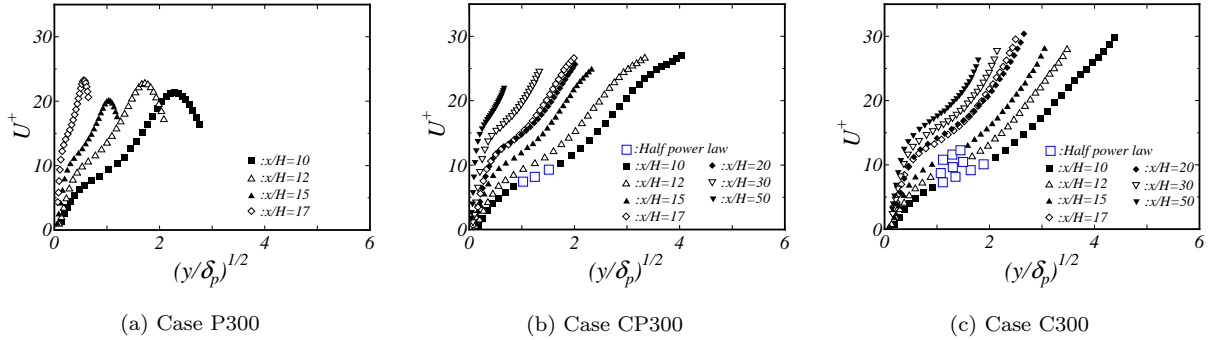
Figure 7: Mean velocity profiles on sections with adverse pressure gradient

(a) Case P300

(b) Case CP300

(c) Case C300
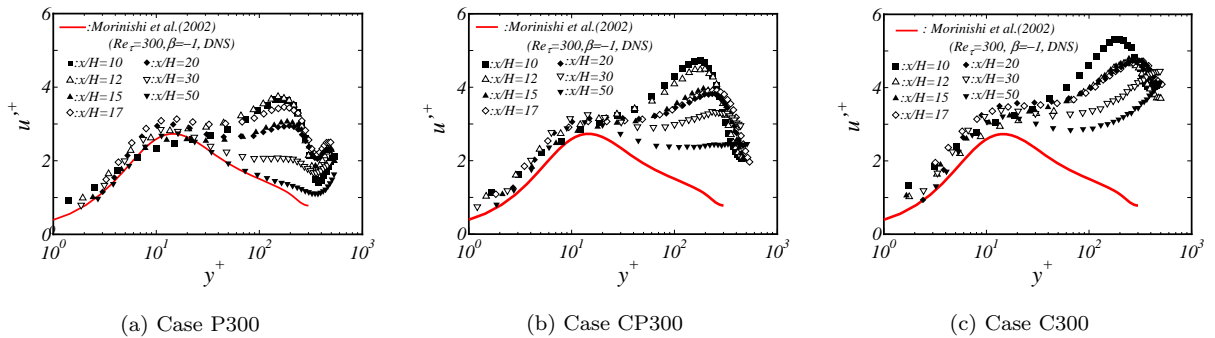
Figure 8: Turbulence intensity profiles

(a) Case P300

(b) Case CP300

(c) Case C300